Coherent Modelling of Backscatter and Propagation of Precipitation

Thomas Börner[*], David H.O. Bebbington[*], Madhukar Chandra[**]

[*] University of Essex, Dept. of Electronic Systems Engineering, Wivenhoe Park, Colchester CO4 3SQ, Essex, UK
Phone / Fax: +44-1206-87-2819 / -2900, Email: thomas.boerner@dlr.de, david@essex.ac.uk

[**] DLR, Deutsches Zentrum für Luft- und Raumfahrt e.V., Institut für Hochfrequenztechnik und Radarsysteme, Oberpfaffenhofen, D-82234 Weßling, Germany
Phone / Fax: +49-8153-28-2313 / -1449, Email: madhu.chandra@dlr.de

Abstract

In order to improve knowledge about scattering processes and their effects on the backscattered signal, accurate modelling of radar backscatter is required. In this paper we present a stochastic, coherent and fully-polarimetric scattering model which simulates the propagation of an electromagnetic wave through a medium containing raindrops of various sizes, shapes and orientations and calculates the backscattered signal. Some simulation examples will show the potential of the model with regard to understanding and predicting various effects and scenarios.

1. Introduction

The model populates an illuminated volume with raindrops, calculating the scattering properties of individual drops, taking into account various drop size distributions (DSD) [1-5] related to certain rainfall rates, orientation, temperature and movement (fall speed). The complex propagation constant, which is a 2×2-matrix in the polarimetric case, is calculated by applying the extinction theorem to the modelled coherent average of the stochastically generated forward scattering amplitudes. The extinction is strongly dependent on the drop size distribution and hence the rain rate.

One important application of the model is the simulation of a movement of the scatterers and the impact on the derivation of the elements of the polarimetric scattering matrix. Because radars cannot transmit and receive two polarisations at the same time, there is a time delay between the measurement of the individual elements, resulting in decorrelation due to relative drop motions. We will use the model to show qualitative and quantitative effects of such movements on the coherence of the scattering matrix. Especially when it comes to coherence matrices, basis transformations and/or coherent decompositions, those effects might play a non-negligible role and have to be quantified.

A second application of the model is to predict the effects of precipitation not only for weather radar systems, but for airborne and spaceborne SAR-systems as well. Strong rainfall might influence the results of classifications based on coherent target decompositions as well as results obtained using polarimetric interferometry, etc. We will show first results to demonstrate the usefulness of the model, particularly in combination with other radar systems.

2. Volume containing Raindrops

The measured polarimetric backscatter from a medium containing raindrops is sensitive to their size, shape, density, orientation and dielectric properties. In order to model the backscatter from a defined volume we first have to know the number of raindrops in the volume and the distribution of their sizes. For our model we use three well-established DSDs, i.e. from Marshall-Palmer [5], Ulbrich [3,4] and Haddad et al. [1,2], all of them having the general form of a Gamma distribution

$$N(D) = N_0 D^{\mu} \exp(-\Lambda D) \qquad (1)$$

with the drop diameter $0 < D < D_{max}$, three parameters (N_0, Λ, μ) and the dimensions [$mm^{-1}m^{-3}$] (special care has to be taken here, because the authors do not always express the drop diameters in mm, but also in cm). The Marshall-Palmer DSD is an exponential distribution with $\mu = 0$. The parameters particularly depend on the rain rate R [mm/h].

The number of raindrops N_{int} for a defined rain rate R in a defined interval of diameters ΔD per unit volume is derived by integrating $N(D)$

$$N_{int}(D, \Delta D) = \int_{D}^{D+\Delta D} N(D)\, dD \qquad (2)$$

For our model we will populate a volume V with drops of distinct sizes $D_{min} < D_i < D_{max}$, defined as the average drop diameter in a fixed interval ΔD and $i = 1,\ldots,n$ (number of distinct drop diameters). Hence the total number of raindrops in a volume V is

$$N_{tot} = V\sum_{i=1}^{n} N_{\text{int}}(D_i, \Delta D) \quad (3)$$

3. The Model

We consider a radar sensing a region of rain as shown in Figure 1. The illuminated volume V is increasing with the range distance R from the radar. Let the distance from the radar to the first range gate containing raindrops be R_0, the length of each range gate be r_0 and the angular beam width be Ω. The volume V_n of each range gate is then

$$V_n = \frac{r_0}{3}\left(g_n^2 + g_n g_{n+1} + g_{n+1}^2\right) \quad (4)$$

with $$g_n = (R_0 + r_0(n-1))\tan\Omega \quad (5)$$

Hence we can populate every volume V_n according to the number of drops due to equation (3), giving each drop a random position (r_i, ψ_i, θ_i), where ψ_i is the elevation angle and θ_i is the azimuth angle.

The backward scattering of an incident wave in the horizontal (h) and vertical (v) basis can be described as

$$\begin{bmatrix} E_v \\ E_h \end{bmatrix}_{scat} = \frac{\exp(i\underline{k}\underline{R})}{R}\begin{bmatrix} S_{hh} & S_{hv} \\ S_{vh} & S_{vv} \end{bmatrix}\begin{bmatrix} E_v \\ E_v \end{bmatrix}_{inc} = \frac{1}{R}\begin{bmatrix} M_{hh} & M_{hv} \\ M_{vh} & M_{vv} \end{bmatrix}\begin{bmatrix} E_v \\ E_v \end{bmatrix}_{inc} \quad (6)$$

where $\underline{k}$ is the wavevector. The elements of the scattering matrix **S** are related to the coherent combination of backward and forward scattering amplitudes $f_{h,v}(D)$ of each drop, calculated by the FIM method [6]. Since every drop may have a different canting angle ϕ_i and tilt angle $\Psi_i = \psi_i + \Delta\psi$ with regard to the direction of propagation, we have to derive a 2×2 complex matrix

$$\tilde{\mathbf{S}} = \begin{bmatrix} \cos\phi_i & \sin\phi_i \\ -\sin\phi_i & \cos\phi_i \end{bmatrix}\begin{bmatrix} f_{\Psi_i,h} & 0 \\ 0 & f_{\Psi_i,v} \end{bmatrix}\begin{bmatrix} \cos\phi_i & -\sin\phi_i \\ \sin\phi_i & \cos\phi_i \end{bmatrix} \quad (7)$$

containing the scattering amplitudes of each drop, depending on drop size, orientation and direction of scattering (backward, forward). Note that f is originally only derived for symmetric orientation of the drop and hence the cross-channels are zero, whereas after tilting and rotating the drop there will be a contribution in the cross-channels as well.

Since $\underline{k}$ and $\underline{R}$ are parallel, the vector product can be replaced by $\mathbf{k}R$, where $\mathbf{k}$ is now called the propagation constant, which is a 2×2 complex matrix in the polarimetric case. If the length of the range gate r_0 is small (in the order of some wavelengths λ) the forward propagation through a single gate with volume V_n can then be obtained by using [7]

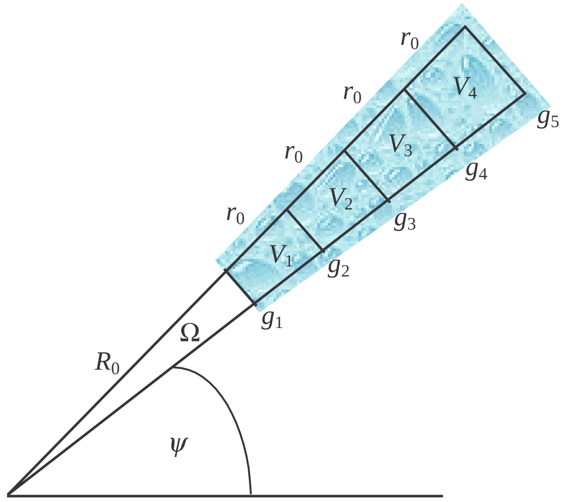

Fig. 1: Geometry of the model

$$\mathbf{k}_n = k_0\mathbf{I} + \frac{2\pi}{k_0 V_n}\int_{V_n}\tilde{\mathbf{S}}_{forw}\,dV_n = \frac{2\pi}{\lambda}\mathbf{I} + \frac{\lambda}{V_n}\sum_{i=1}^{N_{tot,n}}\tilde{\mathbf{S}}_{forw} \quad (8)$$

where $k_0 = 2\pi/\lambda$ is the wavenumber in free space and **I** is the 2×2 unit matrix. The matrix **M** describing the coherent backscatter of the nth range gate can then be written as

$$\mathbf{M}_n = \left(\prod_{i=1}^{n-1}\exp(2ir_0\mathbf{I})\mathbf{k}_i\right)\cdot\left(\sum_{j=1}^{N_{tot,n}}\left(\exp(2ir_j\mathbf{I})\mathbf{k}_n\right)\cdot\tilde{\mathbf{S}}_{back,j}\right) \quad (9)$$

where the product is the two-way propagation through all the n-1 previous range gates, and the sum is the coherent sum of backscatter contributions from each drop, taking into account the individual two-way propagation through the nth range gate.

Going from **M** to the reflectivity $Z_{hh,vv}$ requires sample averaging (indicated by $\langle\ldots\rangle$) and scaling. Since historically Z is expressed in [mm^{6}m^{-3}] we have to multiply by $(10^3)^6 = 10^{18}$, because all variables used in the model are expressed in [m]. Hence

$$Z_{hh,vv}^{(n)} = \frac{10^{18}}{4}\frac{|K_w|^2\lambda^4}{\pi^5}\left\langle|\mathbf{M}_n|^2\right\rangle \quad (10)$$

with $$K_w = \frac{\varepsilon_w - 1}{\varepsilon_w + 2} \quad (11)$$

where ε_w is the relative dielectric permittivity of water at a given temperature.

Now consider a vertical movement of the drops due to their terminal velocity v assumed as [8]

$$v(D) = 3.778\cdot D^{0.67} \quad ;\ (D \text{ in [mm] and } v \text{ in [m/s]}) \quad (12)$$

The position (r_i,ψ_i) of the ith rain drop in the nth range gate will then change by Δz to (r'_i,ψ'_i) in the following way

$$\Delta z(D_i) = v(D_i)\cdot \Delta t$$
$$\psi_i' = \arctan\left(\left(1-\frac{\Delta z(D_i)}{(R_0+nr_0+r_i)\sin\psi_i}\right)\tan\psi_i\right) \quad (13)$$
$$r_i' = \frac{(R_0+nr_0+r_i)\sin\psi_i - \Delta z(D_i)}{\sin\psi_i'} - (R_0+nr_0)$$

where Δt is the time between the initial and the end positions. As for now we are not taking into account any possible changes in orientation of the drops while falling. This certainly needs further investigation.

4. Simulations and Results

We are using C-band (5.635 GHz) and an elevation of 5 degrees for all the simulations shown in this chapter. The first simulations have been carried out in order to show that the model produces reasonable numbers compared to results known from literature. One of the most common relations used for extracting rain rate from radar data is *R-Z*. The according simulation is shown in Figure 2 and agrees with examples found in literature [4,9], as well as the attenuation throughout the medium (Figure 3).

Now consider that the rain drops are not perfectly aligned, giving them a random orientation with varying tilt and canting angles. If we then transform the scattering matrices **M** from the *h*-*v*-basis to the Pauli-basis and derive the measures Entropy H and alpha-angle α from the coherence matrix (target decomposition theory and algorithm can be found in [10]) we get the results shown in Figures 4 (a)-(d). Briefly the Entropy H is a measure for the randomness of the scattering process, with values ranging between 0 (deterministic scattering process) and 1 (random scattering process), whereas α is a measure for the "type" of scattering, ranging from 0° to 90° (α = 0°: isotropic surface; α = 45°: isotropic dipole; α = 90°: isotropic double-bounce; values in between denote anisotropic scattering). The measures for Figure 4 (a) and (b) have been derived without any movement of the rain drops, assuming that the elements of the scattering matrix are all measured at the same time. Figure 4 (c) and (d) instead show the result derived with a time delay of 4 ms between measuring the pairs of elements (M_{hh},M_{hv}) and (M_{vh},M_{vv}) (applying eq. (13) to the latter pair), which is a realistic assumption when considering that the radar sends out a pulse in *h*-polarisation, receiving *h* and *v* simultaneously, then sending the next pulse in *v*, receiving *h* and *v*, choosing a time delay of 4 ms between the outgoing *h* and *v* pulse for the results in Figure 4. The shape of a rain drop varies from spherical to oblate with increasing drop-size, so the average rain drop is an oblate particle. From Figure 4 (b) we see that the highest α-angle is obtained when no rotation is applied, but with increasing random tilt and canting variation α decreases, whereas the opposite effect occurs for the Entropy H (Figure 4 (a)). Due to the increasing random orientation of the drops the integrated backscatter approaches spherical behaviour,

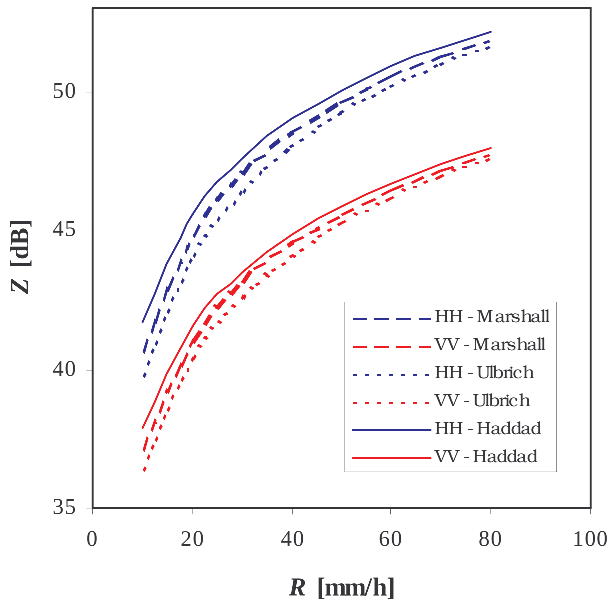

Fig. 2: Relation of rain rate R and reflectivity Z_{hh}, Z_{vv} for various DSDs.

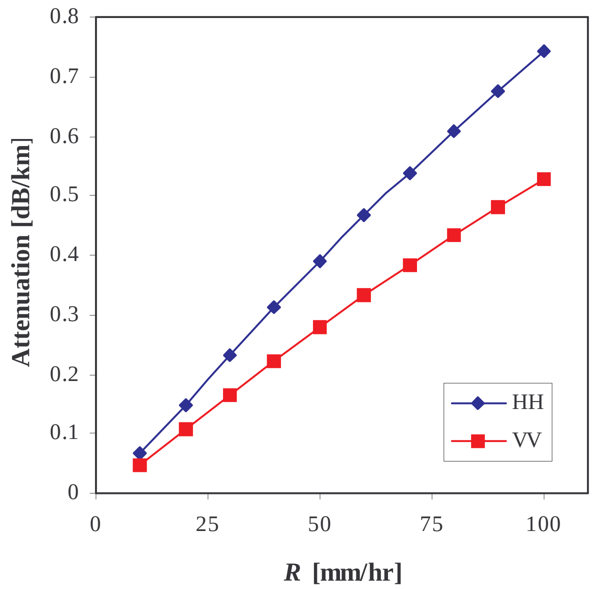

Fig. 3: Specific attenuation depending on rain rate R, using the Marshall-Palmer DSD.

but with high Entropy. A time delay of 4 ms and the associated vertical movement of the drops has a huge effect on both, Entropy and α (Figure 4 (c) and (d)). The Entropy is only low if no change in orientation is applied, showing nearly the same value as without any time delay, but increases fast up to very high numbers when adding some randomness. α is overall much higher than before. We do not yet fully understand why the Entropy is nearly zero when no randomness in orientation is applied, but increases very fast when applying only small changes in tilt angle. A reasonable explanation could be that the DSDs are usually producing a

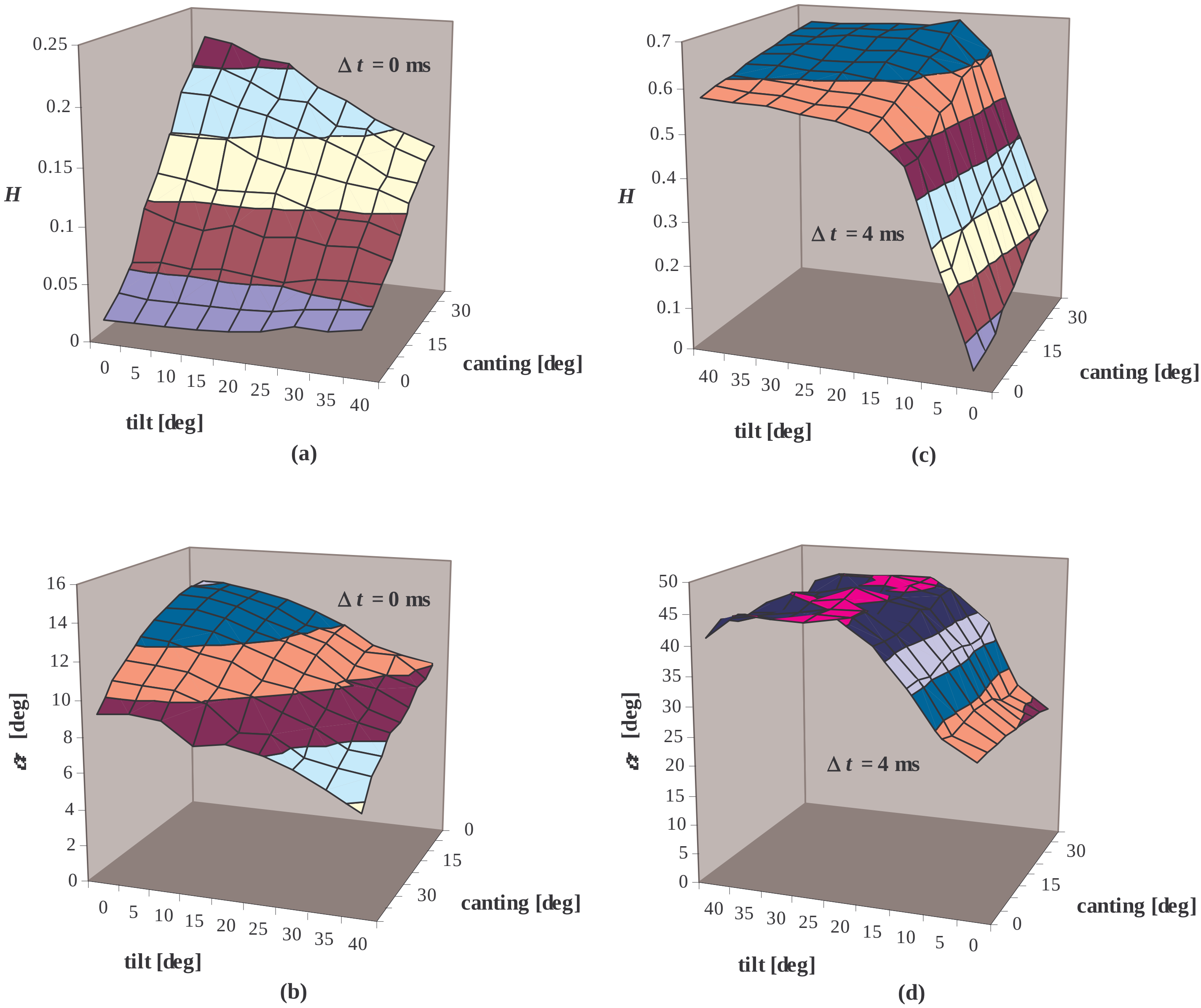

Fig. 4: (a) Entropy *H*, no time delay, **(b)** α-angle, no time delay, **(c)** Entropy *H*, Δt = 4 ms, **(d)** α-angle, Δt = 4 ms. Please read the axis labels carefully, because they are sometimes in reverse order to improve the 3-D view!

huge amount of very small drops, which are nearly spherical, and only a small number of huge drops, which are more oblate and therefore anisotropic scatterers. However, the difference between scattering amplitudes of drops with D = 1mm and drops with D = 4mm is about 10^3, so the influence of the large drops on the Entropy can be very huge compared to the small drops, even if their number is much smaller. If there is no randomness and all drops are aligned, then the Entropy can be very low. But if the randomness in orientation increases, the influence of the anisotropic large drops comes in rapidly with a huge impact on the Entropy and α as well. This effect is interesting and needs to be investigated more carefully in the future.

The amount of change due to Δt certainly depends on the length of the delay, as shown in Figure 5. Both H and α converge to a maximum, which is reached at about Δt = 4 ms, being $\alpha_{max} \approx 45°$ and $H_{max} \approx 0.6$.

The propagation throughout the altered medium is also different, but only slightly, because it is not affected by the phase changes of the scatterers. It only depends on the integrated complex scattering amplitudes, and those only vary because of a different elevation angle. Hence the effects of propagation are expected to be very small, and in fact the results for H and α do not show any dependence of the range gate and the previous attenuation/extinction.

5. Conclusions

In the previous chapter we showed that our model results agree with other models and experimental data found in the literature and that it can be used to calculate reflectivity and attenuation for different rain rates and drop size distributions. However, since we are taking into account the scattering of each drop, computing the propagation along a huge distance (several km) is very time-consuming. Existing other models (for example [11]) can be used more easily to obtain results for those cases.

The advantage of our model is to deal with coherent and non-coherent effects introduced by a movement or change in orientation of individual scatterers. We have shown that only slight vertical movements can affect observables like Entropy and α-angle to a huge amount. Further investigations will also have to take into account changes in orientation, which might occur due to wind turbulences or collisions between drops. Therefore a physical understanding of such movements has to be established and implemented into the model.

Since the propagation effects on the coherence of the scattering seem to be very small, the impact on other radar systems as SAR might be negligible, because those systems are particularly sensing deterministic targets, which usually do not move or change significantly. Hence an Entropy-α based classification should still work well, even if there is a layer of rain in between the sensor and the target. Special care should be taken when looking at targets like forest canopies or crops, because wind and rain can cause those scatterers to move rather quickly with a non-negligible impact on the obtained observables.

6. Acknowledgements

The authors acknowledge funding under the EU TMR programme, contract EC FMRX-CT 98-0211.

7. References

[1] Z.S. Haddad, S.L. Durden, and E. Im, "Parameterizing the Raindrop Size Distribution," *J. Appl. Meteorol.*, vol. 35, pp. 3-13, 1996.

[2] Z.S. Haddad, D.A. Short, S.L. Durden, E. Im, S. Hensley, M.B. Grable, and R.A. Black, "A New Parameterization of the Rain Drop Size Distribution," *IEEE Trans. Geosci. Remote Sensing*, vol. 35, pp. 532-539, May 1997.

[3] C.W. Ulbrich, "Natural Variations in the Analytical Form of the Raindrop Size Distribution," *J. Appl. Meteorol.*, vol. 22, pp. 1764-1775, 1983.

[4] C.W. Ulbrich and D. Atlas, "Rainfall Microphysics and Radar Properties: Analysis Methods for Drop Size Spectra," *J. Appl. Meteorol.*, vol. 37, pp. 912-923, 1998.

[5] J.S. Marshall and W. Palmer, "The Distribution of Raindrops with Size," *J. Meteorol.*, vol. 5, pp. 165-166, 1948.

[6] A.R. Holt, N.K. Uzunoglu and B.G. Evans, "An Integral Equation Solution to the Scattering of Electromagnetic Radiation by Dielectric Spheroids and Ellipsoids," *IEEE Trans. Ant. Prop.*, vol. 26, pp. 706-712, 1978.

[7] N.K. Uzunoglu, B.G. Evans and A.R. Holt, "Scattering of Electromagnetic Radiation by Precipitation Particles and Propagation Characteristics of Terrestrial and Space Communication Systems," *Proc. IEE*, vol. 124, pp. 417-424, 1977.

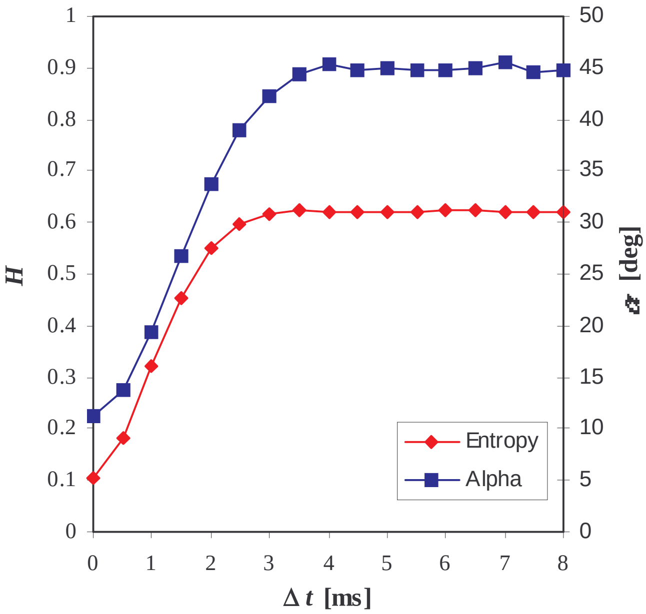

Fig. 5: Δ*t* dependence of *H* and α, canting and tilt angle variation is 20°.

[8] J.D. Doviak and D.S. Zrnic, *Doppler Radar and Weather Observations*, 2nd ed., San Diego, CA: Academic, 1993.

[9] R.L. Olsen, D.V. Rogers and D.B. Hodge, "The aR^b Relation in the Calculation of Rain Attenuation," *IEEE Trans. Ant. Prop.*, vol. 26, pp. 318-329, 1978.

[10] S.R. Cloude and E. Pottier, "A Review of Target Decomposition Theorems in Radar Polarimetry," *IEEE Trans. Geosci. Remote Sensing*, vol. 34, no. 2, pp. 498-518, 1996.

[11] R. McGuinness, D.H.O. Bebbington, A.R. Holt, "Modelling Propagation Effects in the use of S-band Polarisation-diversity Radars," *IEE Proc.*, vol. 134, Pt. H, no. 5, 1987.